Journal of Population Therapeutics & Clinical Pharmacology

RESEARCH ARTICLE
DOI: 10.47750/jptcp.2023.30.04.026

Redox-Sensitive Targeted Doxorubicin-Loaded Chitosan-based Nanoparticles to Treat Breast Cancer

Mahsa Babaei[1] , Soheila Kashanian[2,3*], Zahra Salemi[4], Hossein Zhaleh[5]

[1] Department of Biology, Faculty of Science, Razi University, Kermanshah, Iran

[2]Faculty of Chemistry, Sensor and Biosensor Research Center (SBRC), Razi University, Kermanshah, Iran

[3] Nanobiotechnology Department, Faculty of Innovative Science and Technology, Razi University, Kermanshah, Iran

[4] Department of Biochemistry, Arak University of Medical Sciences, Arak, Iran

[5] Substance Abuse Prevention Research Center, Institute of Health, Kermanshah University of medical science, Kermanshah, Iran

***Corresponding author:** Soheila Kashanian, Faculty of Chemistry, Sensor and Biosensor Research Center (SBRC), Razi University, Kermanshah, Iran, Email: kashanian_s@yahoo.com

Submitted: 10 January 2023; Accepted: 12 February 2023; Published: 10 March 2023

ABSTRACT

The positive charge of chitosan (Cs) polymer has limited its utilization as a carrier for doxorubicin (DOX). Herein, a Cs derived by covalent linkage to L-Cysteine (L-Cys) was offered to reduce the positive charge of the polymer and to enhance the DOX entrapment efficiency (EE). Hence, the hyaluronic acid-targeted DOX-loaded Cs-Cys nanoparticles (HA/Cs-CysNPs-DOX) were synthesized as a redox-responsive carrier for intracellular delivery of DOX. At first, the Cs-CysNPs-DOX was synthesized by ion-gelation technique, after which HA was attached by electrostatic interaction as a targeting agent. Ultimately, they were characterized in terms of size, zeta potential, EE, drug loading (DL), and morphology. HA/Cs-CysNPs-DOX based on the novel copolymers displayed an appropriate EE for DOX and redox-stimuli drug release. The hemolysis assay proved the safety and hemocompatibility of the NPs, which confirms their intravenous application. In vitro drug release indicated high stability in physiological conditions with a glutathione (GSH) dependence drug release. The cytotoxicity and apoptosis of HA/Cs-CysNPs-DOX were also studied by investigating MCF-7 cells with various concentrations and times. A considerable cytotoxicity enhancement was displayed for HA/Cs-CysNPs-DOX compared to Cs-CysNPs-DOX and free DOX, while no cytotoxicity effects were found for free NPs. The caspase-3 activity showed that apoptosis was enhanced by raising the concentration of DOX, and the free NPs did not exhibit any caspase-3 activity. Overall, the developed HA/Cs-CysNPs-DOX displayed a high potential for targeted therapy and effective applications in biomedical investigation.

Keywords: *Breast cancer; Chitosan; Doxorubicin; Hyaluronic acid; Redox-sensitive*

This article is distributed under the terms of the Creative Commons Attribution-Non Commercial 4.0 International License. ©2021 Muslim OT et al.

INTRODUCTION

Chemotherapy is a critical cancer treatment procedure, but insolubility, non-specificity, wide biological distribution, short half-life, non-bioavailability, and cytotoxicity of chemotherapy drugs restrict their effective treatment application [1]. So, because of its side effects on normal cells and tissues, a drug delivery system (DDS) with appropriate DL and EE is crucial for targeting the tumor cells and delivering the anticancer drugs into the tumor environment [2]. NPs as the DDS have advantages such as protecting the drugs and increasing the retention time, improving the solubility of hydrophobic drugs, targeted delivery to the desired tumor site and expanding the therapeutic effect, controlling the drug release, maintaining the drug concentration in the body, and multiple drug delivery possibilities to acquire synergistic therapeutic results [3]. Various approaches have been used to improve the ability of NPs to penetrate the tumor tissue and prolong its existence in blood circulation. Several strategies have also been employed to enhance the selectivity of NPs to a specific tissue, one of which is applying functionalization with target tissue-specific ligands, such as HA, which precisely binds to CD-44 receptors and promotes cellular uptake via endocytosis [4, 5].

Biopolymer-based NPs have appropriate characteristics, such as biocompatibility, biodegradability, cost-effectiveness, and eco-affability, which make them an excellent choice for drug formulation and delivery in pharmaceutical industry [6]. Among biopolymers, Cs is a natural amino polysaccharide with cationic nature derived from the deacetylation of chitin, which is known for non-toxicity, biodegradability, and biocompatibility, and therefore has been extensively studied in nanobiomedical experiments [7]. Cs has two functional groups,-OH and -NH2, which generate the potential for hydrogen and covalent bond formation and provide more capability for chemical modifications of the polymer and the production of various derivatives with unique characteristics [8]. These functional moieties play a critical role in the solubility of Cs, and also, amino groups are protonated at a low pH and cause a positive charge to the polymer. Due to this cationic nature, it triggers a vigorous electrostatic interaction with negatively charged components of mucus [9].

By integrating the stimuli-responsive bonds in the polymeric component of the NPs, the release behavior of the drug can be prompted in response to the endogenous triggers of the tumor tissues, increase the local release of the drug in the target tissue, and reduce the side effects [10]. NPs with stimuli-responsive linkages can alter their physicochemical characteristics such as surface properties, size, and morphology in the specific triggers that induce local drug release by responding to endogenous triggers of tumor cells [11]. Diverse stimuli-responsive NPs are organized for controlled drug delivery [12]. Among them, redox responsivity is a special property because the concentration of GSH as a reduction factor is about 10 mM in the cytosol, while it is about 2 μM in the blood plasma, and the highly hypoxic tumor microenvironment contains four times higher levels of GSH than normal tissues [13, 14]. L-Cys is an amino acid that can be included in the redox reaction by its sulfhydryl group. It is oxidized by removing hydrogen from the thiol group, and the disulfide bond is produced [15]. Therefore, the incorporation of L-Cys into the structure of NPs turns them into redox-responsive systems that cause rapid and selective drug release just in response to a reduced condition in a controlled manner.

DOX is a standard cationic anticancer drug approved by the food and drug administration (FDA) for the treatment of diverse types of cancer, but DOX, like other classes of chemotherapy drugs, has many disadvantages that restrict its clinical application, including high cytotoxicity, low bioavailability, and the high dose required [16]. Thus, many studies have evaluated DOX encapsulation to improve drug utilization with low side effects simultaneously [17]. Utilization of NPs with cationic surface charges has been preferred for drug delivery to enhance cell adhesion and cellular uptake by attraction to negatively charged cell membranes [18]. As mentioned, DOX is cationic in nature and its entrapment in a Cs polymer with a high density of positively charged amine groups is the central problem, so the Cs can be chemically modified to overcome its limitations as a drug delivery vehicle [19].

In the present study, Cs biopolymer was coupled to L-Cys (Cs-Cys co-polymer), and the resulting derivation was utilized to develop DOX-loaded Cs-CysNPs (Cs-CysNPs-DOX) as a redox-

J Popul Ther Clin Pharmacol Vol 30(4):e267–e282; 10 March 2023.
This article is distributed under the terms of the Creative Commons Attribution-Non Commercial 4.0 International License. ©2021 Muslim OT et al.

responsive vehicle. In DOX delivery by Cs-CysNPs-DOX, the presence of the thiol group in L-Cys enhances the solubility of the NPs and induces oxidation and reduction responsivity, which leads to the rapid and selective release of the drug, specifically in response to reducing the triggers of tumor cells microenvironments. Thus, Cs-CysNPs-DOX is prepared via the ionic gelation technique and then targeted by HA via electrostatic interactions between HA and the positive charges of the CS-CysNPs surface (HA/Cs-CysNPs-DOX). Ultimately, the physicochemical properties, cumulative release of DOX, hemolysis test, cellular cytotoxicity, and cellular uptake efficiency are assessed. All examinations are performed to consider the potential of the HA/CS-CysNPS-DOX as a device for efficient intracellular delivery of DOX.

2. MATERIALS AND METHODS

2.1. Chemicals

In this work, the chemicals utilized consisted of 5,5-dithiobis(2-nitrobenzoicacid) (DTNB, Ellman's reagent), DOX, Cs, L-Cys, sodium triphosphate (TPP); phosphate-buffered saline (PBS); GSH; sodium borohydride (NaBH4); HA, 1-ethyl-3-(3-dimethyl aminopropyl) carbodiimide hydrochloride (EDC), N-hydroxysuccinimide (NHS), 3-(4,5-dimethylthiazol-2-yl)-2,5-diphenyltetrazolium bromide (MTT), non-essential amino acid (NEAA, Sigma), L-glutamine, penicillin, and streptomycin. Fetal bovine serum (FBS), MCF-7 cell lines as the human breast cancer cells, Dulbecco's modified eagle medium (DMEM), and LDH cytotoxicity detection kit were purchased from GIBCO Invitrogen (Grand Island, NY). All other reagents, chemicals, and solvents were of chemical or analytical grade as required. The deionized water was used for the preparation of all aqueous solutions.

2.2. Preparation of Cs-Cys co-polymer

The synthesis of Cs-Cys co-polymer was done via the conjugation of the carboxylic acid groups of L-Cys to the CS amine backbone (Fig. 1). According to Mazzotta et al., the best Cs to L-Cys ratio was 1:2, which produced a copolymer with a high percent of disulfide bond and also smaller NPs [20]. For this purpose, 35 mg of Cs was dissolved in 35 mL of 1% (v/v) acetic acid to obtain a 1% (w/v) Cs solution. Separately, L-Cys was agitated for one hour in the presence of EDC in the deionized water to activate its carboxylic groups. Then, it was added dropwise to the 1% Cs solution under magnetic stirring (Cs/Cys ratio 1:2). The pH of the reaction mixture was adjusted to 5 by 0.5 M NaOH. Afterward, the mixture was stirred overnight in the dark at 25 °C. The final product was purified by dialysis for three days (via a 12 kDa dialysis bag). The dialysis was performed against 5 mM HCl, 5 mM HCl containing 1% NaCl, and 1 mM HCl, respectively. The purified copolymers were lyophilized and stored at 4 °C. The final products were subjected to 1H nuclear magnetic resonance (NMR) to confirm L-Cys conjugation to Cs.

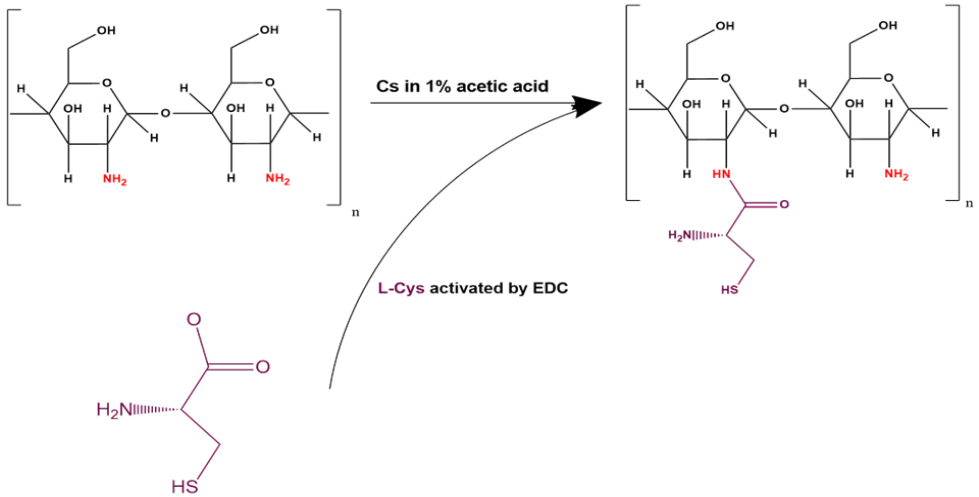

FIG. 1: Synthesis protocol of Cs-Cys copolymer by EDC activation

J Popul Ther Clin Pharmacol Vol 30(4):e267–e282; 10 March 2023.
This article is distributed under the terms of the Creative Commons Attribution-Non Commercial 4.0 International License. ©2021 Muslim OT et al.

2.3. Elman Test

The number of thiol groups immobilized on the Cs-Cys copolymer was defined by Ellman's test, which quantifies free thiol groups. First, 0.5 mg of copolymer and control sample were dissolved in 500 µL of 0.5 M phosphate buffer pH 8.0. Then, 500 µL of Ellman's reagent (3 mg of DTNB in 10 mL of 0.5 M phosphate buffer pH 8.0) was added, and the samples were incubated at room temperature for 2 hours. Ultimately, the samples were transferred into the microplate, and absorbency at 450 nm was measured by a microplate reader (Epoch™ 2 Microplate Spectrophotometer, BioTek Instruments, Inc). The L-Cys calibration curve was employed to estimate the percent of the thiol groups of the copolymer.

The number of disulfide bonds within the copolymer was analyzed by the following procedure. First, 0.5 mg of the copolymer was hydrated in 1 mL of 0.05 M phosphate buffer with pH 8.0 for 30 minutes. Then, 600 µL of fresh 3% sodium borohydride solution were added to the copolymer solution, and the mixture was incubated for 2 hours in a water bath at 37 ± 0.5 °C under magnetic stirring. After that, 500 µL of 1 M HCl and 100 µL of acetone were added and stirred for 5 minutes. Finally, 200 µL of 0.5% DTNB in 0.5 M phosphate buffer pH 8.0 and 1 mL of 1 M phosphate buffer pH 8.5 were added and incubated for 15 min at 25 °C. The samples were poured into the 96-well microplates to measure free sulfhydryl groups. The number of disulfide bonds was estimated by subtracting the number of free thiols calculated by the Ellman's method from the total thiol groups within the copolymer [21].

2.4. Preparation of DOX-loaded Cs-CysNPs

Cs-CysNPs-DOX was synthesized by the ionic gelation method, as referred by several researches with modifications, and the NPs were formed by the ionic interaction of TPP as an anionic cross-linking agent with the cationic copolymer. Briefly, 5 mg of Cs-Cys copolymer was dissolved in 4 mL of 1% (v/v) acetic acid (1.25 mg/mL). DOX was added to the copolymer solution at 0.3:1 drug: copolymer ratio (w:w) before adding the TPP solution. The pH of the resulting solution was adjusted to 5 with NaOH solution. After that, the alkaline TPP solution (1 mg/mL) was added to the above solution dropwise under a 200-rpm stirring speed at room temperature (Cs-Cys/TPP ratio 6:1) [22]. Cs-CysNps-DOX was assembled immediately and spontaneously. The effect of Cs and TPP concentrations on the particle size, size distribution, and cumulative release of DOX was analyzed. Selected formulations with appropriate particle size and narrow size distribution with sustained release of the DOX were employed to target the experiments.

2.5. Synthesis of the HA-targeted Cs-CysNps-DOX

HA-targeted Cs-CysNPs-DOX was synthesized by previously reported procedures [23]. In this technique, the positive charges of the amine groups of Cs on the surface of Cs-CysNPs-DOX are crosslinked with the anionic HA. For this purpose, 600 µL HA (0.05 mg/mL of 15000KD) was added to 3 mL Cs-CysNPs-DOX solution dropwise, without employing a cross-linking agent, and stirred for 20 min. Thereafter, HA/Cs-CysNPs-DOX were characterized by the size and zeta potential of NPs.

2.6. Characterization of NPs

Particle size and zeta potential

The hydrodynamic diameter and zeta potential of Cs-CysNPs-DOX and HA/Cs-CysNPs-DOX at 25.0 ± 0.1 °C were investigated by dynamic light scattering (DLS) (Nanoptic 90 Plus - Bettersize Instruments Ltd.) and Zetasizer (Malvern Instruments Ltd., Worcestershire, UK). The samples were evaluated 3 times, and the outcomes were expressed as mean ± standard deviation (SD).

2.7. Morphology

Scanning electron microscopy (SEM) was employed to determine the morphology of NPs at an operative voltage of 25 kV by TESCAN BRNO-Mira3 LMU, Brno, Czech Republic.

2.8. Drug Entrapment Efficiency

The EE and DL of DOX were evaluated by the dialysis technique, and the ultraviolet absorbance at wavelengths of 480 nm was analyzed by a plate reader spectrophotometer (Epoch™ 2 Microplate Spectrophotometer, BioTek Instruments, Inc) [24]. The EE was calculated by the following equation, and the highest EE of different formulations was selected:

This article is distributed under the terms of the Creative Commons Attribution-Non Commercial 4.0 International License. ©2021 Muslim OT et al.

$$\text{EE \%} = \frac{\text{DOX tot} - \text{DOX free}}{\text{DOX tot}} * 100 \quad (1)$$

Additionally, DL was determined by the following equation:

$$\text{DL \%} = \frac{\text{Weight of the entrapped DOX}}{\text{Total weight of HA/Cs-CysNPs-DOX}} * 100 \quad (2)$$

2.9. In vitro Redox-responsive drug release

Drug release from Cs-CysNPs-DOX and HA/Cs-CysNPs-DOX was determined by the dialysis bag diffusion procedure at 37 ◦C in different release media. Briefly, aliquots of NPs were poured into the dialysis bags (12 kDa cut-off) and soaked in PBS pH 7.4 in the presence and absence of 10 mM GSH. The systems were kept under magnetic stirring. At designed time intervals, 500 µL of release medium was withdrawn from each sample for the absorbance analysis at 480 nm, and 500 µL fresh buffers were added to keep the sink condition. All the measures were triplicated, and the outcomes were consistent with the standard error of ±5%.

2.10. Hemolysis assay of drug-free HA/Cs-CysNPs

The biocompatibility of the HA/Cs-CysNPs was analyzed by the hemolysis assay. For this purpose, fresh human blood samples were collected from a healthy donor, and EDTA was operated to stabilize them. After centrifugation, blood samples were dissolved in 0.9% normal saline solution, and 2% w/v red blood cells (RBC) suspension was prepared. Then, 1.25 mL of RBC were suspended in normal saline and distilled water as the negative and positive controls, respectively. Different concentrations of HA/Cs-CysNPs (0.15 mL) were incubated with 2% RBC or normal saline at 37.0 °C for 3 h. Finally, after the centrifugation of the samples at 1500 rpm for 15 minutes, the hemolytic ratio (HR) was evaluated by measuring the supernatant absorbance at 540 nm using equation 3:

$$\text{HR} = \frac{\text{Absorbance sample} - \text{Absorbance } (-) \text{ control}}{\text{Absorbance } (+) \text{ control} - \text{Absorbance } (-) \text{ control}} \quad (3)$$

2.11. Cell Culture

MCF-7 cells were cultured in appropriate media, DMEM, and complemented with 10% FBS, 1% NEAA, 2 mM L-glutamine, 100 µg/mL streptomycin, and 100 IU/mL penicillin. Afterward, they were incubated at 37 °C in 5% CO2. Then, they were trypsinized by trypsin-EDTA 0.25% and subcultured in 24-well culture plates at a density of 1×104 cells/well. The cells were washed with PBS at pH 7.4 and were categorized into four groups based on their incubation treatment media; first: free NPs, second: DOX, third: Cs-CysNPs, and fourth: HA/Cs-CysNPs.

2.12. MTT Assay

Cell viability was studied by performing the MTT assay. At first, 15×103 cells were poured into a 96-well plate, following which 200 µL of DMEM media containing 0.2% BSA was added. After incubation for 24h, 200 µL of treatment media was added to the wells. The cells were individually incubated with various treatment media i.e, free NPs, DOX, Cs-CysNPs, and HA/Cs-CysNPs in various concentration (i.e., 0, 25, 50, 100, 200, 500, 750, and 1000 nM) for 48. Finally, the supernatant from each well was taken, and 50 µL of MTT solution (5 mg/mL) was added and incubated for 3 hours. Furthermore, the samples were taken from the supernatant of each well and dissolved to formazan crystals. Then, dimethyl sulfoxide was added for 30 minutes at 25 °C. The optical density of each sample was analyzed at 570 and 630 nm by an ELISA reader.

The cell proliferation inhibition was quantified for each concentration by the following formula:

$$\text{Cell viability} = \frac{\text{Absorbance of the treated cells}}{\text{Absorbance of the untreated cells}} \times 100 \quad (4)$$

The cell viability was described as the means of at least three different examinations ± SD.

2.13. LDH assay

LDH assay was used to evaluate cell toxicity. For this reason, 2 × 105 cells/well were cultured in a 24-well plate for 12 h. Cells were individually incubated for 24 h with various treatment media of free NPs, DOX, Cs-CysNPs, and HA/Cs-CysNPs (i.e., 0, 25, 50, 100, 200, 500, 750, and

This article is distributed under the terms of the Creative Commons Attribution-Non Commercial 4.0 International License. ©2021 Muslim OT et al.

1000 nM). Then, conditioned media of cells were transferred to a fresh 96-well plate with the LDH assay reagent. After 30 min, the ELISA reader was employed to detect the LDH activity by colorimetric assay at 490 nm.

2.14. Caspase-3 assay

MCF-7 cells were cultured in various treatment media, treated with different concentrations of DOX and varius NPs formulations (i.e., 0, 25, 50, 100, 200, 500, 750, and 1000 nM), and incubated for 24 and 48 h. Afterwards the cells were treated, the caspase-3 activity of their lysates was quantified by a caspase activity colorimetric assay utilizing a plate reader. Data were analyzed from three independent investigations [25].

2.15. Statistical Analysis

Quantitative data were expressed as the mean of three results ±standard deviation (SD). One-way analysis of variance (ANOVA) followed by t-test was used for statistical analysis and a value of $p < 0.05$ was considered.

3. RESULTS AND DISCUSSION

3.1. Characterization of Cs-Cys Co-polymer

Recently, new multi-functional CsNPs have been designed and investigated for redox-stimuli response and potential administration in targeted therapy. NPs with redox-responsive properties are particularly demanding in the intracellular delivery of drugs for cancer treatment. Notably, in this study, Cs as one of the biodegradable biopolymers was selected as the initial material, due to its straightforward modification of the functional amino groups, which enhances the potential of tumor targeting. However, Cs is a cationic polymer and does not have good efficiency for loading the cationic DOX. So, the Cs derivate was constructed via the conjugation of Cs to the L-Cys amino acid, which improved the hydrophilic nature of the co-polymer and enhanced the DOX loading in CsNPs. On the other hand, L-Cys is one of the reagents used for the immobilization of thiol groups on primary amino groups of Cs and induced redox responsivity to NPs. In this study, L-Cys was functionalized and coupled to the Cs backbone through amide bonds. During the synthesis of the thiolated polymers, the pH of the environment prevents disulfide bond formation by air oxidation. In this pH range, disulfide bond formation is not desirable because the concentration of thiolate anion is low [26]. This indicates that the thiol groups of L-Cys are easily oxidized by air after the synthesis and purification steps to form inter- and intra-molecular disulfide bonds. These disulfide bonds can eventually be cleaved under reducing conditions. In addition, the size of NPs is affected by the presence of disulfide linkages in the polymer, and the smaller NPs are created by enhancing the disulfide content. Thus, in this study, the Cs/Cys ratio of 2:1 was considered for co-polymer synthesis [20]. The Cs-Cys co-polymer procedure of synthesis is summarized in Fig. 1, and the chemical arrangement was represented by a 1H-NMR investigation.

The co-polymer structure was verified by the 1H-NMR spectrum, as shown in Fig. 2. In the Cs-Cys proton spectrum, the peak δ1.94 = CH3 corresponds to the acetyl group of Cs, δ2.89 = CH, carbon 2 of Cs, δ3.5-3.8 = CH + CH2, carbon 3-6 of Cs, and δ4. 6 = CH, carbon 1 of Cs. Furthermore, Cs-Cys represented a methylene spectrum at δ3.01, which characterizes the methylene bond to the thiol group because Cs does not contain methylene and also this characteristic peak [27]. Various peaks were also detected in Cs-Cys, which is presumably due to the presence of L-Cys groups. As a result, the formation of an amide bond was demonstrated by the 1H NMR spectrum.

This article is distributed under the terms of the Creative Commons Attribution-Non Commercial 4.0 International License. ©2021 Muslim OT et al.

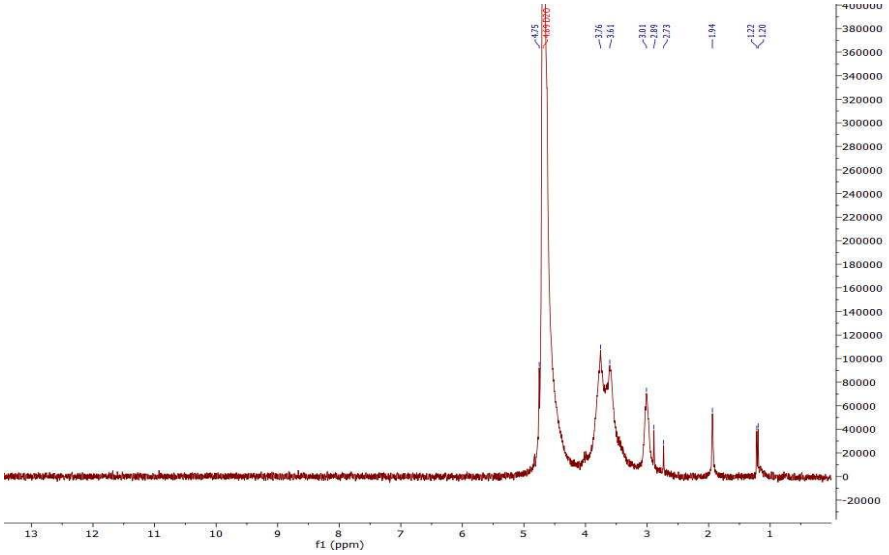

FIG. 2 NMR peaks of Cs-Cys copolymer

3.2. Elman's test

Eventually, Elman's test was utilized to estimate the number of free thiol groups and disulfide bonds in Cs-Cys co-polymer. In our synthesized Cs-Cys co-polymer, the disulfide content was calculated to be 83.29%.

3.3. Characterization of NPs

Size and zeta potential

Here, the redox-responsive NPs were synthesized by the ion gelation technique, in which the NPs are assembled via the electrostatic interaction of a positively charged Cs-Cys co-polymer with a negatively charged cross-linker, TPP. The synthesis of NPs was carried out in various concentrations of co-polymer and TPP. Drug EE and the appearance of solutions were analyzed. The best ratio of Cs-Cys/TPP with a suitable opalescent appearance without colloidal grains as well as high EE was fixed for the formulation. The preferred formulation (1.25 Cs (mg/mL): 1 TPP (mg/mL)) was homogeneous and very stable over a long period (more than four weeks, at room temperature and in the dark). Physicochemical characteristics are a critical factor from a pharmaceutical perspective and are considered an essential element in anticipating in vivo performance. Therefore, the developed NPs were characterized in terms of particle size, polydispersity index (PDI), and zeta potential.

The size of NPs affects their drug release properties and penetration into tumor tissues. Many publications have documented that various solid tumors exhibit hypervascular permeability and impair lymphatic drainage. Because of this, NPs significantly penetrate the tumor microenvironment via the EPR effect, which is typically operated by NPs with 100–400 nm. Table. 1 shows that the average hydrodynamic diameters are 177.71 nm and 165.10 nm for Cs-CysNPs-DOX and the HA modification of Cs-CysNPs-DOX, respectively. The 12.61 nm reduction in the size of the NPs is because of the electrostatic interaction of the negative HA with the surface of the CsNPs. Therefore, the structure of the NPs is compacted, and their size is decreased. The small sizes of the Cs-CysNps-DOX and HA/Cs-CysNps-DOX (<400 nm) make them suitable for use as drug delivery carriers. These results are in good agreement with those evaluated by SEM analysis.

The final formulations of NPs represented positive zeta potential values between +30 ± 1.4 and +35.9 ± 0.36 mV (Fig. 3). The positive charge of NPs is associated with the unbounded H of Cs, which displays the high stability of the NPs suspensions. Furthermore, the NPs with positive zeta potential enhanced cellular uptake by electrostatic interactions with an anionic member of the cells and improved reposition via negative channels of the cell membrane. In the case of HA/Cs-CysNPs-DOX, reducing the positive charge after HA interaction proves that HA effectively interacts with the surface amine groups of CsNPs. In addition, the size

This article is distributed under the terms of the Creative Commons Attribution-Non Commercial 4.0 International License. ©2021 Muslim OT et al.

distributions of the NPs are reasonable, which is displayed by PDI values lower than 0.3, as reported in Table. 1.

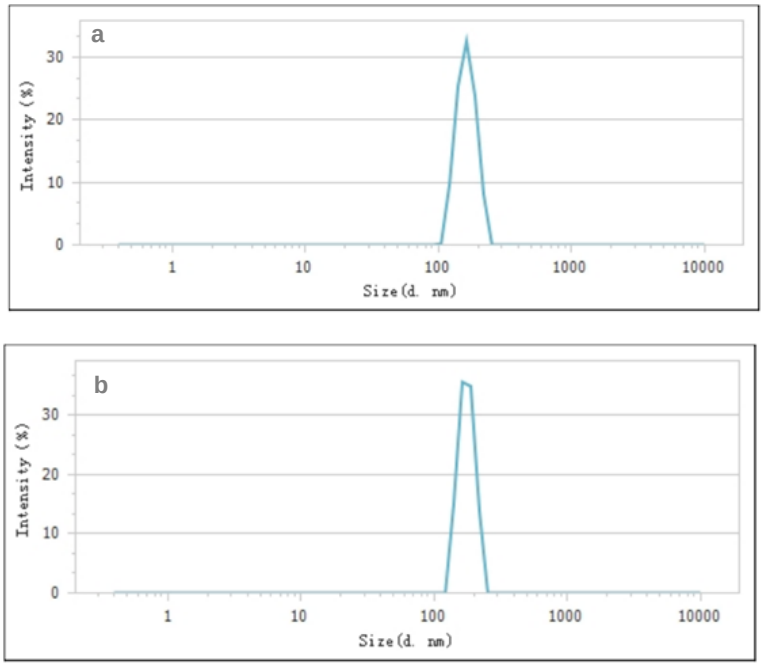

Diam(nm)	Size
D10	122.44
D20	130.06
D30	137.68
D40	144.96
D50	151.84
D60	158.72
D70	166.44
D80	177.34
D90	188.24
D100	220.19

Diam(nm)	Size
D10	135.07
D20	144.73
D30	151.01
D40	157.29
D50	163.58
D60	170.89
D70	178.32
D80	185.74
D90	198.85
D100	220.19

FIG. 3: Size distribution of a) Cs-CysNPs-DOX and b) HA/Cs-CysNPs-DOX

TABLE 1: Characterization of Cs-CysNPs-DOX and HA/Cs-CysNPs-DOX

Sample	Size (nm)	PDI	Zeta potential (mv)	Physical appearance
Cs-CysNPs-DOX	177.71	0.079	+35.2	Opalescent suspension
HA/Cs-CysNPs-DOX	165.10	0.260	+30.6	Opalescent suspension

3.4. Morphology

The morphology of NPs was investigated by SEM analysis [28]. A few NPs were detected in the SEM image, which indicates agglomeration or contamination during the sample preparation [29]. As shown in Fig. 4, the mean hydrodynamic diameters ranged from 150 nm to 177.1 nm. In addition, SEM analysis confirmed that the particles have a spherical shape, with a smooth surface.

This article is distributed under the terms of the Creative Commons Attribution-Non Commercial 4.0 International License. ©2021 Muslim OT et al.

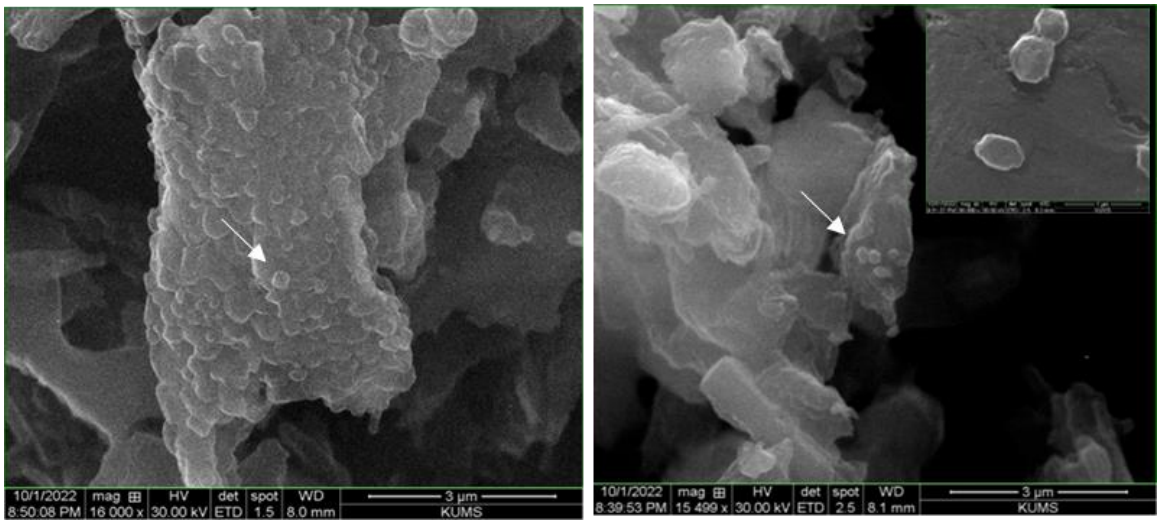

FIG. 4: The SEM images of DOX-loaded NPs

3.5. Determination of drug EE and DL

The Cs-CysNPs-DOX was synthesized by the ionic gelation technique. At a pH of approximately 4.8, the amine groups of Cs are protonated and electrostatically interacted with negatively charged TPP. On the other hand, DOX, as a positively charged drug, prevents the formation of NPs by creating an ionic interaction with TPP. Therefore, these non- specific interactions are a critical issue for loading DOX into CsNPs, as a positively charged polymer.

In a recent study in 2018, Zare et al. synthetized CsNPs for DOX with only up to 23% EE [30]. In another study by P. Katuwavila, DOX-loaded CsNPs encapsulated only 65% of DOX [31]. Further, M. A. Abd El-Ghaffar loaded DOX in CsNPs and Cs-glutamate to improve EE. Their results demonstrated that as the DOX concentration was raised, the EE increased to reach the highest concentration of 69% for copolymer/DOX and 30% for CsNPs/DOX [32]. In 2021, Huang et al. utilized oligosaccharide (CSO)/indomethacin (Indo) NPs for DOX delivery to enhance its solubility, as the hydrophobic drug was alkalized in the aqueous medium. Their findings indicated that EE and DL were 70–80% and 5-7%, respectively [33]. In the present study, the EE of DOX was 77.2% and 76.1% for Cs-CysNPs-DOX and HA/Cs-CysNPs-DOX, respectively. Therefore, by employing the Cs-Cys copolymer, EE has increased to a great extent compared to the previous studies in which only Cs was used [34-36]. DL was estimated to be 13.55 ± 0.129% and 12.59 ± 0.069% for Cs- CysNPs-DOX and HA/Cs-CysNPs-DOX, respectively, with an enhancement compared to the previous publication.

3.6. In vitro release studies

HA/Cs-CysNPs-DOX are administrated by intravenous injection into the blood circulation. They are transferred into the tumor microenvironment by the EPR effect, and afterward, they are taken up by the cells through the CD-44 receptor [37]. Accordingly, appropriate stability in blood circulation and extracellular tumor environment are critical purposes for the design of ideal drug delivery carriers, which can preserve the drug to release it rapidly and entirely into the cancer cells by stimuli [38]. In this study, to ensure the redox-responsive properties of the designed NPs, the release profile investigations were performed at PBS 0.01 M with pH 7.4, in the absence and presence of 10 mM GSH, to mimic the physiologic environment and interior of the tumor cells, respectively [39]. The GSH concentration in the intracellular tumor cells is around four-fold higher than that of the healthy cells. Intracellular GSH levels are also 100–1000-fold higher in cancer cells than in extracellular levels [23, 40]. Therefore, GSH is selected as the reducing agent to consider the redox-responsive characterization of NPs. The profile release of DOX for HA/Cs-CysNPs-DOX and HA/Cs-CysNPs-DOX is represented in Fig. 5. A gradual slow release of below 37% is shown in PBS at pH 7.4, which indicates reasonable

This article is distributed under the terms of the Creative Commons Attribution-Non Commercial 4.0 International License. ©2021 Muslim OT et al.

stability in healthy cells with a little drug leakage in blood circulation. In contrast, at 10 mM GSH concentration, a more rapid drug release occurs due to the disulfide bond cleavage in the structure of NPs and shows 60% drug release in the first 4 h and up to 88% after 24 h. On the other hand, HA/Cs-CysNPs-DOX can be rapidly disassembled by GSH in the highly reductive condition of cancer cells, which causes a fast DOX release and inhibits cancer growth. Consequently, these results confirm the GSH responsivity of both Cs-CysNPs-DOX and HA/Cs-CysNPs-DOX and verify their great potential for intracellular cancer DOX delivery.

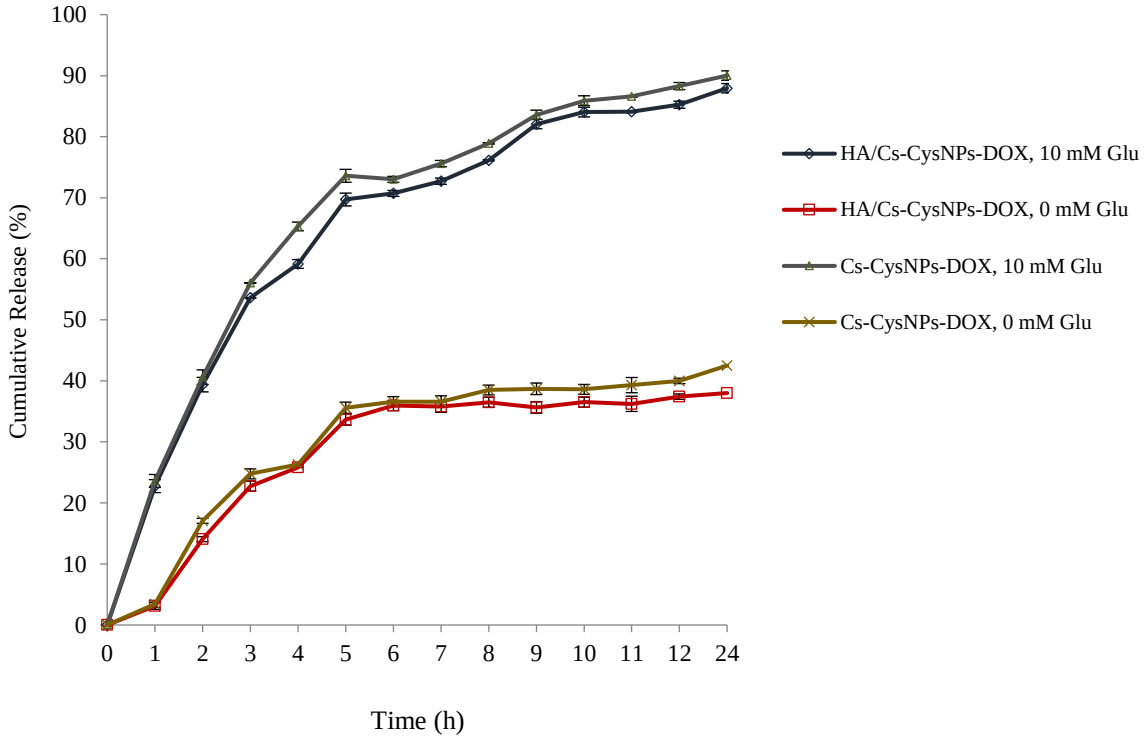

FIG. 5: The in vitro release profile of DOX from different NPs in PBS 0.01 M pH 7.4, in the presence and absence of GSH 10 mM at 37 ◦C. The amount of DOX release in PBS in the presence of GSH 10 mM at each point was statistically different (* $p < 0.05$) from that evaluated in the absence of GSH

3.7. Hemolysis assay

The amount of red blood cell lysis and hemoglobin released by HA/Cs-CysNPs is determined by hemolysis assay. Thus, the hemolysis assay is a critical test for evaluating NPs in terms of biocompatibility and safety after injection. Thus, less than 10% hemolysis by NPs is reasonable for injection into the blood circulation [41, 42]. As shown in Fig. 6, the amount of hemolysis affected by HA/Cs-CysNPs is only 3.23%, even at the highest concentration (i.e., 3.0 mg/mL). This result demonstrates the essential blood safety and biocompatibility of HA/Cs-CysNPs for intravenous injection. Overall, we can conclude that all the HA/Cs-CysNPs compositions (including Cs-Cys copolymer, TPP, and HA) are biocompatible and not toxic to blood and other biological samples.

This article is distributed under the terms of the Creative Commons Attribution-Non Commercial 4.0 International License. ©2021 Muslim OT et al.

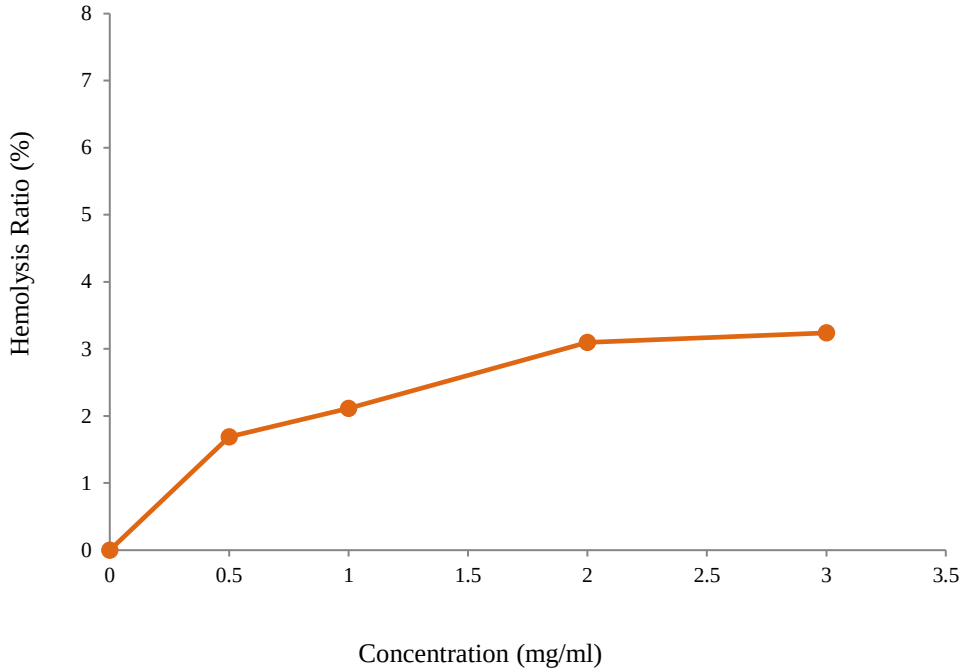

FIG. 6: Hemolysis assay analysis of HA/Cs-CysNPs for intravenous injection

3.8. MTT assay

The results of MTT assay display the cell viability of MCF-7 cells at different concentrations of NPs. As indicated in Fig. 7, both formulations can cause cell growth inhibition in a dose-dependent manner. As expected, due to the overexpression of CD44 receptors on the MCF-7 cells, HA/Cs-CysNPs-DOX displayed the highest inhibition effects on the cell growth compared to Cs-CysNPs-DOX, and also both formulations indicated a more reasonable effect than free DOX. In sum, we can conclude that the NPs formulations do not have any cytotoxic effect on MCF-7 cells up to 1000 nM of NPs. In addition, the percentages of the growth inhibition for HA/Cs-CysNPs-DOX, Cs-CysNPs-DOX, DOX, and NPs are 100%, 84%, 76%, and 1.5%, respectively, in 1000 nM after 48 h treatment (Fig. 7). These results prove the definite effects of HA/Cs-CysNPs-DOX on the inhibition of CD-44 positive cell growth to deliver and release DOX into the cells.

J Popul Ther Clin Pharmacol Vol 30(4):e267–e282; 10 March 2023.
This article is distributed under the terms of the Creative Commons Attribution-Non Commercial 4.0 International License. ©2021 Muslim OT et al.

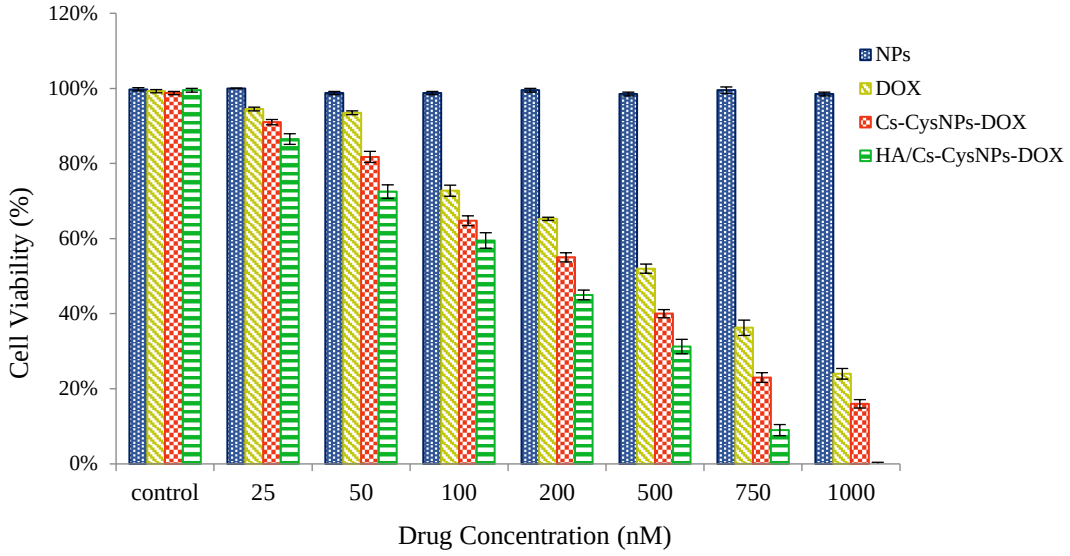

FIG. 7: In vitro cytotoxicity of different concentrations of NPs against MCF-7 breast cancer cells

3.9. LDH assay

LDH assay is done to confirm the results of MTT assay. After the cell is damaged and the membrane is disturbed, the LDH level, as a stable cytosolic enzyme, is enhanced [43]. So, the LDH assay indicated the cytotoxicity% of the cells by evaluating the LDH levels. As expected, the free NPs formulation did not show any cytotoxic effect (Fig. 8). By contrast, cell cytotoxicity was raised by increasing the concentration of DOX. Moreover, the cytotoxic effect revealed the dose-dependent manner for drug-loaded NPs formulations, in which HA/Cs-CysNPs-DOX had a higher cytotoxic effect than Cs-CysNPs-DOX and free DOX.

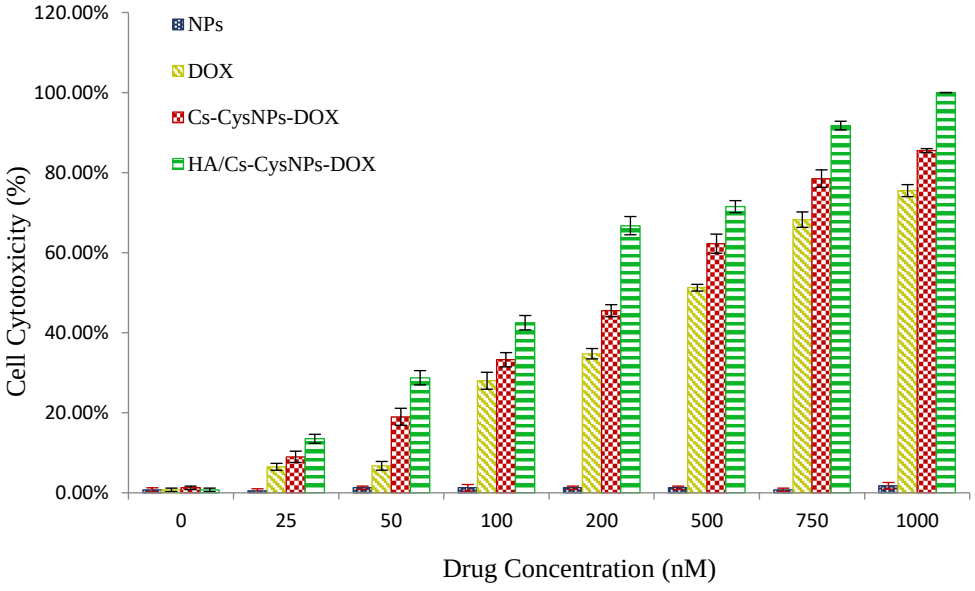

FIG. 8: DOX cytotoxicity measured by the LDH assay in MCF-7 cells. All data are displayed as mean ± S.E.M ($p < 0.05$)

J Popul Ther Clin Pharmacol Vol 30(4):e267–e282; 10 March 2023.
This article is distributed under the terms of the Creative Commons Attribution-Non Commercial 4.0 International License. ©2021 Muslim OT et al.

3.10. Caspase-3 assay

Activation of Caspase 3, as an essential component in cell death, enhances the cell cytotoxicity and apoptosis [44]. As depicted in Fig. 9, DOX enhances Caspase-3 activity and apoptosis in a dose-dependent manner. Furthermore, the free NPs do not have any caspase-3activation. However, HA/Cs-CysNPs-DOX and Cs-CysNPs-DOX show increased Caspase-3 activity compared to free DOX, in which HA/Cs-CysNPs-DOX as a targeted carrier had a higher caspase-3 activation effect than non-targeted Cs-CysNPs-DOX. On the other hand, Caspase-3 activation occurs in HA/Cs-CysNPs-DOX, Cs-CysNPs-DOX, DOX, and NPs, respectively.

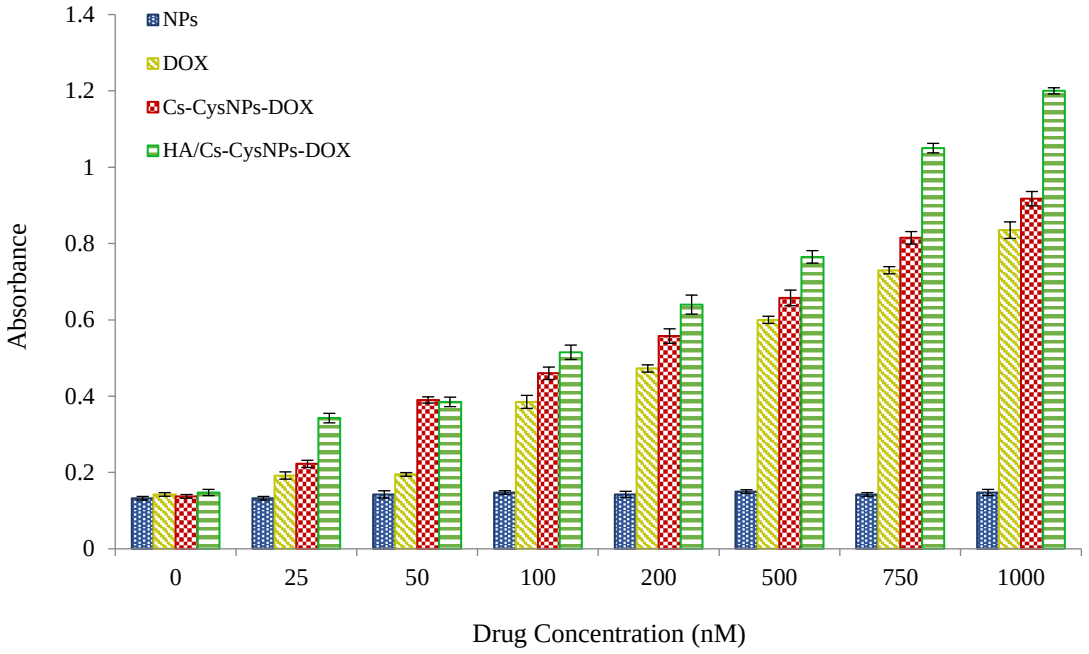

FIG. 9: Quantification of Caspase 3 activity by the Caspase colorimetric assay kit. All data are indicated by mean ± S.E.M ($p < 0.05$)

4. CONCLUSION

The positive charge of Cs is considered the main challenge in the encapsulation of DOX into CsNPs. For this purpose, L-Cys is employed to introduce disulfide bonds into the copolymer backbone to enhance the EE of DOX and induce redox-sensitive properties in NPs. Hence, we developed the multifunctional HA/Cs-CysNPs-DOX, which targeted the cancer cells by HA, as a CD-44 receptor ligand, and released DOX under redox-responsive conditions. The results displayed that the interaction of HA affects the size and zeta potential. The zeta potential reduction from 35.0 to 30.0 mV revealed that HA successfully interacted with NPs. On the other hand, these zeta potentials display high stability in blood circulation and reduce the non-specific interaction with serum proteins. The EE and DL of the structure represent suitable NPs with resealable drug entrapment. The in vitro drug releases of HA/Cs-CysNPs-DOX offers appropriate stability in physiological conditions with a redox-sensitive drug release in the cancer simulation environment. The hemolysis assay proved the safety and hemocompatibility of the NPs, which confirms their intravenous application. The in vitro assay indicated that free multifunctional targeted NPs do not have any cytotoxic effects on MCF-7 cells, while HA/Cs-CysNPs-DOX displayed prominent cytotoxicity and apoptotic effect on the overexpression of CD44 cells and MCF-7 compared to non-targeted NPs and free DOX. In conclusion, the developed NPs have a high potential for targeted cancer therapy, and their reduction sensitivity offers effective applications in biomedical investigations. Moreover, future in

This article is distributed under the terms of the Creative Commons Attribution-Non Commercial 4.0 International License. ©2021 Muslim OT et al.

vivo investigations are required to confirm their efficacy.

5. FUNDING

No funding was received for conducting this study.

6. ETHICS DECLARATIONS

Conflict of interest

The authors declare that they have no conflict of interest.

REFERENCES

1. Alqosaibi AI (2022) Nanocarriers for anticancer drugs: Challenges and perspectives. Saudi J Biol Sci. 29:103298. https://doi.org/10.1016/j.sjbs.2022.103298
2. Wang C, Zhang Z, Chen B, Gu L, Li Y, Yu S (2018) Design and evaluation of galactosylated chitosan/graphene oxide nanoparticles as a drug delivery system. J Colloid Interface Sci. 516:332-41. https://doi.org/10.3390/polym14112287
3. Wang S-Y, Hu H-Z, Qing X-C, Zhang Z-C, Shao Z-W (2020) Recent advances of drug delivery nanocarriers in osteosarcoma treatment. J Cancer. 11:69-82. https://doi.org/10.7150/jca.36588
4. Bajracharya R, Song JG, Patil BR, Lee SH, Noh H-M, Kim D-H, Kim G-L, Seo S-H, Park J-W, Jeong SH, Lee CH, Han H-K (2022) Functional ligands for improving anticancer drug therapy: current status and applications to drug delivery systems. Drug Deliv. 29:1959-70. https://doi.org/10.1080/10717544.2022.2089296
5. Chiesa E, Greco A, Riva F, Dorati R, Conti B, Modena T, Genta I (2022) CD44-Targeted Carriers: The Role of Molecular Weight of Hyaluronic Acid in the Uptake of Hyaluronic Acid-Based Nanoparticles. Pharmaceuticals. 15:103. https://doi.org/10.3390%2Fph15010103
6. Vodyashkin AA, Kezimana P, Vetcher AA, Stanishevskiy YM (2022) Biopolymeric Nanoparticles–Multifunctional Materials of the Future. Polymer. 14:2287. https://doi.org/10.3390/polym14112287
7. Jesus S, Marques AP, Duarte A, Soares E, Costa JP, Colaço M, Schmutz M, Som C, Borchard G, Wick P, Borges O (2020) Chitosan Nanoparticles: Shedding Light on Immunotoxicity and Hemocompatibility. Front Bioeng Biotechnol. 8:100. https://doi.org/10.3389/fbioe.2020.00100
8. George D, Maheswari PU, Begum KMS (2020) Cysteine conjugated chitosan based green nanohybrid hydrogel embedded with zinc oxide nanoparticles towards enhanced therapeutic potential of naringenin. React Funct Polym. 148:104480. http://dx.doi.org/10.1016/j.reactfunctpolym.2020.104480
9. M. Ways TM, Lau WM, Khutoryanskiy VV (2018) Chitosan and Its Derivatives for Application in Mucoadhesive Drug Delivery Systems. Polymer. 10:267. https://doi.org/10.3390%2Fpolym10030267
10. Hershberger KK, Gauger AJ, Bronstein LM (2021) Utilizing Stimuli Responsive Linkages to Engineer and Enhance Polymer Nanoparticle-Based Drug Delivery Platforms. ACS Appl Bio Mater. 4:4720-36. https://doi.org/10.1021/acsabm.1c00351
11. Majumder J, Minko T (2021) Multifunctional and stimuli-responsive nanocarriers for targeted therapeutic delivery. Expert Opin Drug Deliv. 18:205-27. https://doi.org/10.1080/17425247.2021.1828339
12. Murugan B, Sagadevan S, Fatimah I, Oh W-C, Hossain MAM, Johan MR (2021) Smart stimuli-responsive nanocarriers for the cancer therapy – nanomedicine. Nanotechnol Rev. 10:933-53. https://doi.org/10.1515/ntrev-2021-0067
13. Xiang Z, Liu M, Song J (2021) Stimuli-Responsive Polymeric Nanosystems for Controlled Drug Delivery. Appl Sci. 11:9541. https://doi.org/10.3390/app11209541
14. Omrani I, Babanejad N, Shendi HK, Nabid MR (2017) Fully glutathione degradable waterborne polyurethane nanocarriers: Preparation, redox-sensitivity, and triggered intracellular drug release. Mater Sci Eng C. 70:607-16. http://dx.doi.org/10.1016/j.msec.2016.09.036
15. Yap WF, Yunus WMM, Yusof NA, Ibrahim NI, Zainudin AA. Characterization and optical properties of L-cysteine/chitosan biocomposite thin film. 2014.
16. Butowska K, Woziwodzka A, Borowik A, Piosik J (2021) Polymeric Nanocarriers: A Transformation in Doxorubicin Therapies. Materials (Basel, Switzerland). 14:https://doi.org/10.3390/ma14092135
17. Wang D, Zhang X, Xu B (2021) PEGylated Doxorubicin Prodrug-Forming Reduction-Sensitive Micelles With High Drug Loading and Improved Anticancer Therapy. Front Bioeng Biotechnol. 9:https://doi.org/10.3389/fbioe.2021.781982
18. Tan ML, Choong PF, Dass CR (2009) Doxorubicin delivery systems based on chitosan for cancer therapy. J Pharm Pharmacol. 61:131-42. https://doi.org/10.1211/jpp.61.02.0001
19. Shakil MS, Mahmud KM, Sayem M, Niloy MS, Halder SK, Hossen MS, Uddin MF, Hasan MA (2021) Using Chitosan or Chitosan Derivatives in Cancer Therapy. Polysaccharides. 2:795-816. https://doi.org/10.3390/polysaccharides2040048

This article is distributed under the terms of the Creative Commons Attribution-Non Commercial 4.0 International License. ©2021 Muslim OT et al.

20. Mazzotta E, De Benedittis S, Qualtieri A, Muzzalupo R (2019) Actively targeted and redox responsive delivery of anticancer drug by chitosan nanoparticles. Pharmaceutics. 12:26. https://doi.org/10.3390%2Fpharmaceutics12010026
21. A. B-S, M.D. H, C.E. K, N. L (2002) Thiolated polymers: Stability of thiol moieties under different storage conditions. Sci Pharm. 70:331-9. https://doi.org/10.3797/scipharm.aut-02-32
22. Helmi O, Elshishiny F, Mamdouh W (2021) Targeted doxorubicin delivery and release within breast cancer environment using PEGylated chitosan nanoparticles labeled with monoclonal antibodies. Int J Biol Macromol. 184:325-38. https://doi.org/10.1016/j.ijbiomac.2021.06.014
23. Rezaei S, Kashanian S, Bahrami Y, Cruz LJ, Motiei M (2020) Redox-Sensitive and Hyaluronic Acid-Functionalized Nanoparticles for Improving Breast Cancer Treatment by Cytoplasmic 17α-Methyltestosterone Delivery. Molecules. 25:1181. https://doi.org/10.3390/molecules25051181
24. Hong Y, Che S, Hui B, Yang Y, Wang X, Zhang X, Qiang Y, Ma H (2019) Lung cancer therapy using doxorubicin and curcumin combination: targeted prodrug based, pH sensitive nanomedicine. Biomed Pharmacother. 112:108614. https://doi.org/10.1016/j.biopha.2019.108614
25. Hassanpour A, Irandoust M, Soleimani E, Zhaleh H (2019) Increasing the anticancer activity of azidothymidine toward the breast cancer via rational design of magnetic drug carrier based on molecular imprinting technology. Mater Sci Eng C. 103:109771. https://doi.org/10.1016/j.msec.2019.109771
26. Kurniawan DW, Fudholi A, Susidarti RA (2015) Synthesis of thiolated chitosan as matrix for the preparation of metformin hydrochloride microparticles. Research in Pharmacy. 2:
27. Arif M, Dong Q-J, Raja MA, Zeenat S, Chi Z, Liu C-G (2018) Development of novel pH-sensitive thiolated chitosan/PMLA nanoparticles for amoxicillin delivery to treat Helicobacter pylori. Mater Sci Eng C. 83:17-24. https://doi.org/10.1016/j.msec.2017.08.038
28. Bhatta A, Krishnamoorthy G, Marimuthu N, Dihingia A, Manna P, Biswal HT, Das M, Krishnamoorthy G (2019) Chlorin e6 decorated doxorubicin encapsulated chitosan nanoparticles for photo-controlled cancer drug delivery. Int J Biol Macromol. 136:951-61. https://doi.org/10.1016/j.ijbiomac.2019.06.127
29. Kahdestani SA, Shahriari MH, Abdouss M (2021) Synthesis and characterization of chitosan nanoparticles containing teicoplanin using sol–gel. Polym. 78:1133-48. https://doi.org/10.1007/s00289-020-03134-2
30. Zare M, Samani SM, Sobhani Z (2018) Enhanced intestinal permeation of doxorubicin using chitosan nanoparticles. Adv Pharm Bull. 8:411. https://doi.org/10.15171/apb.2018.048
31. Katuwavila NP, Perera A, Samarakoon SR, Soysa P, Karunaratne V, Amaratunga GA, Karunaratne D (2016) Chitosan-alginate nanoparticle system efficiently delivers doxorubicin to MCF-7 cells. J Nanomater. 2016:
32. El-Ghaffar A, Ahmed M, Akl MA-A, Kamel AM, Hashem MS (2017) Amino acid combined chitosan nanoparticles for controlled release of doxorubicin hydrochloride. Egypt J Chem. 60:507-18. https://doi.org/10.21608/ejchem.2017.745.1021
33. Huang P-W, Zeng Z-W, Zheng W, Wang H, Wei X-H, Shi S-L (2022) Synthesis, Preparation and Evaluation of Doxorubicin-Loaded Chitosan Oligosaccharide/Indomethacin Nanoparticles. J Clust Sci. 33:795-808. https://doi.org/10.1007/s10876-021-02017-4
34. Di Martino A, Kucharczyk P, Capakova Z, Humpolicek P, Sedlarik V (2017) Chitosan-based nanocomplexes for simultaneous loading, burst reduction and controlled release of doxorubicin and 5-fluorouracil. Int J Biol Macromol. 102:613-24. https://doi.org/10.1016/j.ijbiomac.2017.04.004
35. Pornpitchanarong C, Rojanarata T, Opanasopit P, Ngawhirunpat T, Patrojanasophon P (2020) Catechol-modified chitosan/hyaluronic acid nanoparticles as a new avenue for local delivery of doxorubicin to oral cancer cells. Colloids Surf B. 196:111279. https://doi.org/10.1016/j.colsurfb.2020.111279
36. Alkholief M (2019) Optimization of Lecithin-Chitosan nanoparticles for simultaneous encapsulation of doxorubicin and piperine. J Drug Deliv Sci Technol. 52:204-14. https://doi.org/10.1016/j.jddst.2019.04.012
37. Espinosa-Cano E, Huerta-Madroñal M, Cámara-Sánchez P, Seras-Franzoso J, Schwartz S, Abasolo I, San Román J, Aguilar MR (2021) Hyaluronic acid (HA)-coated naproxen-nanoparticles selectively target breast cancer stem cells through COX-independent pathways. Mater Sci Eng C. 124:112024. http://dx.doi.org/10.1016/j.msec.2021.112024
38. Qiu L, Ge L, Long M, Mao J, Ahmed KS, Shan X, Zhang H, Qin L, Lv G, Chen J (2020) Redox-responsive biocompatible nanocarriers based on novel heparosan polysaccharides for intracellular anticancer drug delivery. Asian journal of pharmaceutical sciences. 15:83-94. https://doi.org/10.1016/j.ajps.2018.11.005
39. Xia D, Wang F, Pan S, Yuan S, Liu Y, Xu Y (2021) Redox/pH-Responsive Biodegradable Thiol-Hyaluronic Acid/Chitosan Charge-Reversal Nanocarriers for Triggered Drug Release. Polymer. 13:3785. https://doi.org/10.3390/polym13213785

This article is distributed under the terms of the Creative Commons Attribution-Non Commercial 4.0 International License. ©2021 Muslim OT et al.

40. Sun C, Lu J, Wang J, Hao P, Li C, Qi L, Yang L, He B, Zhong Z, Hao N (2021) Redox-sensitive polymeric micelles with aggregation-induced emission for bioimaging and delivery of anticancer drugs. J Nanobiotechnology. 19:1-15. https://doi.org/10.1186/s12951-020-00761-9
41. Amer Ridha A, Kashanian S, Rafipour R, Hemati Azandaryani A, Zhaleh H, Mahdavian E (2021) A promising dual-drug targeted delivery system in cancer therapy: nanocomplexes of folate–apoferritin-conjugated cationic solid lipid nanoparticles. Pharm Dev Technol. 26:673-81. https://doi.org/10.1080/10837450.2021.1920037
42. Edelman R, Assaraf YG, Levitzky I, Shahar T, Livney YD (2017) Hyaluronic acid-serum albumin conjugate-based nanoparticles for targeted cancer therapy. Oncotarget. 8:24337. https://doi.org/10.18632/oncotarget.15363
43. Yassemi A, Kashanian S, Zhaleh H (2020) Folic acid receptor-targeted solid lipid nanoparticles to enhance cytotoxicity of letrozole through induction of caspase-3 dependent-apoptosis for breast cancer treatment. Pharm Dev Technol. 25:397-407. https://doi.org/10.1080/10837450.2019.1703739
44. Pan Y, Guo M, Nie Z, Huang Y, Peng Y, Liu A, Qing M, Yao S (2012) Colorimetric detection of apoptosis based on caspase-3 activity assay using unmodified gold nanoparticles. Chem comm. 48:997-9. https://doi.org/10.1039/C1CC15407A

This article is distributed under the terms of the Creative Commons Attribution-Non Commercial 4.0 International License. ©2021 Muslim OT et al.